

Carrier excitation by atomic collisions at semiconductor surfaces

P. S. Weiss,* P. L. Trevor, and M. J. Cardillo
AT&T Bell Laboratories, Murray Hill, New Jersey 07974
 (Received 3 March 1988)

We have furthered our understanding of the collisional excitation of carriers at semiconductor surfaces due to hyperthermal neutral-atom scattering, with additional experiments and analyses. We compare the excitation efficiency of Xe to Kr over a range of energies and angles for the InP(100) surface. We extract absolute collisional excitation probabilities using optical carrier excitation to determine carrier recombination rates. We compare excitations on InP(100) to InP(110). The results confirm, on a more quantitative basis, the concept of a rapid equilibration of electronic excitations to a transient local lattice excitation in the vicinity of the atomic impact.

I. INTRODUCTION

Recent experiments in the scattering of hyperthermal rare-gas atoms ($1 < E < 15$ eV) from single-crystal surfaces have revealed a variety of interesting phenomena which relate to the mechanism by which energy is transferred from gases to surfaces.¹⁻⁶ The observations include the excitation of electron-hole pairs (e^-h^+),^{1,2} the sputtering of surface atoms at projectile energies below what is commonly thought to be threshold,^{3,4} and angular scattering distributions with sharp maxima characteristic of the atomic structure of the surface unit cell, despite massive energy loss.^{5,6} In this paper we examine one of these phenomena, the excitation of e^-h^+ , in greater depth. Here, we compare the excitation yields for Xe and Kr at InP(100) and for Xe at the ordered InP(110) surface. We described an optical-excitation experiment designed both to characterize these samples and to derive a more accurate value of the absolute e^-h^+ excitation probability. In addition, using the photoconductance waveforms from the optical-excitation experiments and their associated Fourier transforms, we demonstrate the complex nature of the carrier recombination kinetics.

II. EXPERIMENTAL

The ultrahigh-vacuum molecular-beam surface scattering apparatus used in these studies has been described elsewhere.⁷ A schematic is given in Fig. 1 for reference. Briefly, a Xe, Kr, or Ar beam seeded in H₂ or He was expanded through a 100- μ m aperture in a platinum nozzle that could be heated to 1300°C. The mole fraction of the heavy gas could be continuously varied from 0.1% to 2.0%. The beam was square-wave modulated at 80–1000 Hz for phase-sensitive detection or waveform analysis, or chopped at the same frequencies to give pulses as short as ~ 30 μ sec for time-of-flight (TOF) spectra. After collimation, the beam spot size on the semiconductor single crystal was 1×2 mm². The incident beam energies ranged up to 15.5 eV for Xe, 9.2 eV for Kr, and 5.5 eV for Ar. The measured speed ratios obtained in the rare-gas–H₂ mixtures were typically 13–20 (equal to $v/\Delta v$, full width at

half maximum). The fluxes were calibrated from the scattering chamber partial pressure and referenced to the signal from a flux gauge for pure rare-gas beams expanded through hot nozzles (to prevent clustering).

The crystals used were Fe-compensated semi-insulating InP(100) and InP(110) with Ohmic contacts as described in Ref. 2. The resistivities were typically 10^5 – 10^7 Ω cm. After ion sputtering and annealing InP(100), only weak diffuse diffraction peaks in low-energy electron diffraction (LEED) and HE scattering were observed, indicating that the InP(100) surface was somewhat disordered. Relative

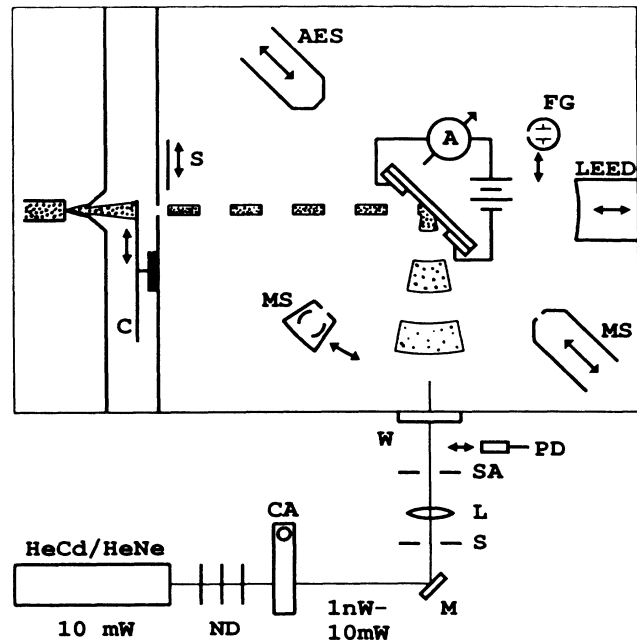


FIG. 1. Schematic of the experimental apparatus. A, ammeter; AES, Auger-electron spectrometer; C, chopper; CA, compensated attenuator; FG, flux gauge; He-Cd, helium-cadmium laser (442 nm); He-Ne, helium-neon laser (632 nm); L, lens; LEED, low-energy electron diffraction; M, mirror; MS, mass spectrometer; ND, neutral-density filters; PD, photodiode; S, shutter; and SA, spatial aperture.

Auger intensities showed the InP(100) to be depleted to various extents of P compared to literature values of nominally stoichiometric surfaces.⁸ In contrast, for InP(110), sharp LEED patterns which accurately reproduce literature I - V characteristics⁸ were obtained, and band bending was reduced to very low values,⁹ suggesting that a substantially well-ordered surface was obtained. Despite these differences in surface order, the measured e^-h^+ yields were about the same for both surfaces for similar incident conditions. The implications of this are discussed below. All experiments discussed here were performed at room temperature.

The electron-hole pair creation efficiency was measured by applying a dc voltage bias across two Ohmic contacts on the front surface of the crystal with the rare-gas beam illuminating a fraction of the region in between. The dc voltages used were typically 1–30 V, leading to bias currents on the order of 10^{-6} A. The peak amplitudes of the transient currents due to the impinging rare-gas atoms were 100 fA–100 pA. The relative efficiencies were obtained by dividing the transient current by the incident flux. The currents were measured on a lock-in amplifier after current-to-voltage conversion, amplification, and nullification of the dc currents.

For different surface conditions resulting from variations in processing, the e^-h^+ yields varied considerably. In order to have some measure of the state of the sample, an optical characterization was developed to measure the carrier recombination kinetics. This made it possible to deduce the efficiency of collisional e^-h^+ creation. Carriers were optically excited using either a He-Ne laser at 632 nm or a He-Cd laser at 442 nm. The incident laser powers were varied from 1 nW to 10 mW using a series of neutral-density filters. The spot size on the crystal was 1 mm. Typically, the laser was opened to the crystal for approximately 10 msec at a repetition rate of less than 1 Hz. A voltage bias was applied across the crystal and a current amplifier was used to convert the induced transient current into a voltage as described above for the molecular-beam e^-h^+ excitation experiment. The signals were recorded as complete waveforms on a multichannel signal averager in summation averaging mode. The measurements were repeated 100 times at each laser power. From the steady-state difference in the number of excess carriers, and the generation rate due to the known laser power absorbed, the minority-carrier lifetime was determined as a function of excess carrier density.¹⁰

III. RESULTS AND DISCUSSION

A. Collisional carrier excitation

The collisional excitation of carriers was measured as a change in the conductivity of a semi-insulating InP(100) or InP(110) crystal as in Ref. 2. The efficiency was studied as a function of incident energy, angle, and atom. The results for Xe and Kr atoms at normal incidence on InP(100) are shown in Fig. 2. The Xe-induced e^-h^+ signals reproduce quantitatively those previously reported in our laboratory.² Note that the Xe was more efficient than Kr at exciting electron-hole pairs at each incident

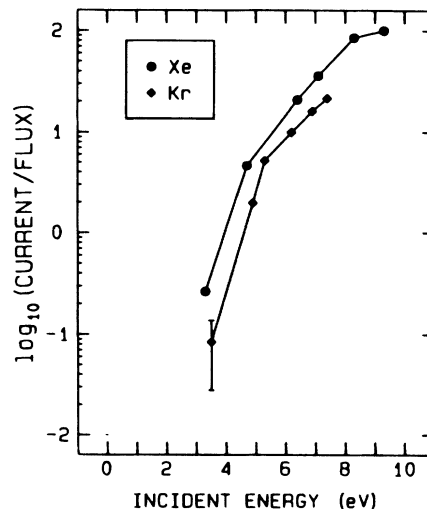


FIG. 2. Relative electron-hole pair excitation efficiency (transient current per incident rare-gas atom) for Xe and Kr atoms at normal incidence to an InP(100) surface. The error bars are smaller than each point, except for the one explicitly shown.

energy. The excitation efficiency was only measured up to 10 eV for Xe, because ion ejection (charge injection) becomes important above this energy and interferes with the e^-h^+ measurement.^{3,4} Up to an energy of 5.5 eV no excitation could be observed for Ar atoms incident on this surface, putting an upper limit on the excitation efficiency which is lower than the efficiency of Xe and Kr at this energy. Typical data for the excitation efficiency as a function of incident angle are shown for Xe atoms at an incident energy of 9.3 eV in Fig. 3 with a maximum at normal incidence. In all cases where e^-h^+ excitations

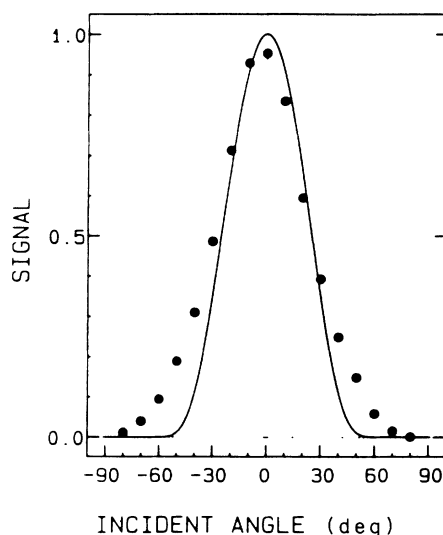


FIG. 3. Electron-hole pair excitation efficiency for Xe atoms at 9.3 eV as a function of incident angle to an InP(100) surface. The solid line shows a fit of the energy dependence of the excitation efficiency to the Xe data of Fig. 2, assuming an exponential dependence on the energy associated with normal motion.

were observed, the yield was orders of magnitude larger than a bulk heating (bolometer) effect due to the impinging atomic beam.

We have previously discussed the excitation of e^-h^+ in terms of a local "hot spot" with rapid electronic equilibration due to the energy transfer of the projectile to the surface. We briefly recall here the conclusions of our previously reported studies of the scattering and energy transfer of Xe, Kr, and Ar atoms at hyperthermal energies from GaAs(110), InP(100), and Ge(100) surfaces.^{4,5} It was found that the energy losses were large in these collisions, and that there was a direct although not strict correlation between the energy loss and the energy associated with motion parallel to the local normal (the local normal was defined as the bisector of the angle made by the incident and reflected atomic velocity vectors). The value of the mean energy transfer was found to be¹¹

$$\Delta E = kE_i \cos^2 \left[\frac{\theta_i + \theta_r}{2} \right], \quad (1)$$

where k is a constant for each rare gas scattered and θ_i and θ_r are the incident and reflected angles with respect to the macroscopic surface normal. The least-squares-fit constants k were $k_{\text{Xe}} = 1.00$, $k_{\text{Kr}} = 0.92$, and $k_{\text{Ar}} = 0.63$.⁴

Combining the results of the scattering experiments with the present results, we plot the excitation efficiency versus the average energy deposited by the atom in the collision (ΔE) in Fig. 4. It is assumed that all scattering is specular ($\theta_i = \theta_r$) so that the energy transfer is just

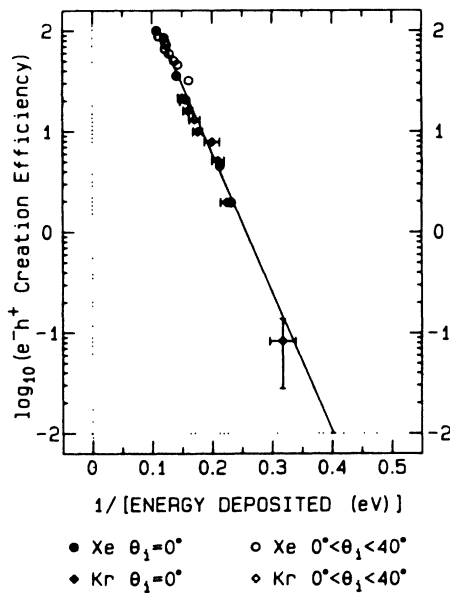


FIG. 4. Electron-hole pair excitation for Xe and Kr atoms on an InP(100) surface as a function of the mean energy deposited in the collision. The solid line is a least-squares fit to the data. Kr atoms are assumed to lose 90% of the energy of Xe atoms at the same energy and angles. Data for angles over 40° always fall above the line shown.

$\Delta E = kE_i \cos^2(\theta_i)$. We note that for low angles of incidence ($\theta_i < 40^\circ$) the excitation efficiency is well fit as exponential in ΔE^{-1} . The deviation at higher angles is expected, because the assumption that the average energy transfer is simply proportional to $kE_i \cos^2\theta_i$ breaks down due to the corrugation of the surface.¹² Subspecular scattering ($\theta_r < \theta_i$) leads to higher energy transfer than $kE_i \cos^2\theta_i$ since these collisions have lower "local incident angles" [see the effect on ΔE in (1)]. In all cases, the excitation efficiency at large angles ($\theta_i \geq 40^\circ$) was higher than the solid lines in Figs. 3 and 4 which represent the assumed exponential dependence on $E_i \cos^2\theta_i$.

This exponential dependence of the efficiency on ΔE^{-1} is consistent with the idea that there is a rapid electronic equilibration with the local lattice energy about the impact of the rare-gas atom—a local thermal hot spot. In the simulations of Xe scattering from GaAs(110) in Ref. 6 it was shown that large energy-transfer collisions were often initially binary, and that the deposited energy was held *transiently* in the target lattice atom and its few closest neighbor atoms. If electronic equilibration is fast compared to the dissipation of energy into the lattice, one expects an exponential dependence on ΔE^{-1} as argued in Ref. 2. Further support is given to this argument by a comparison of the experimental results for Kr and Xe. The Kr data show that the yield depends upon the energy deposited in the collision, and not upon the velocity of the incident particle as might be expected for a process for which a direct coupling to electrons is measured. Since at a given incident energy the velocity is higher for Kr than for Xe, the collision time is shorter. However, the excitation efficiency was lower for Kr than for Xe at each collision energy, implying that a shorter collision time does not increase the excitation yield. We note that the measured excitation yield is the product of the excitation probability and the escape probability of the carrier into the conduction band. It is therefore possible that the statistical behavior observed is primarily a reflection of the carrier escape probability from the local region and not of the initial excitation probability.

B. Optical carrier excitation

1. Carrier recombination lifetime

In order to determine the absolute efficiency of the collisional excitation of electron-hole pairs, a study of the recombination of optically excited carriers was undertaken on the semi-insulating Fe-compensated InP(100) and InP(110) crystals. It was found that the surface electronic properties could easily dominate the bulk-averaged values of resistivity and carrier lifetime.

In the optical-excitation determination of the recombination lifetimes, it was assumed that each absorbed laser photon excited an electron-hole pair with unit efficiency. Both laser photon energies are substantially above the InP direct band gap of 1.35 eV ($E_{\text{He-Ne}} = 1.95$ eV, $E_{\text{He-Cd}} = 2.81$ eV). The carrier generation rate was then the number of photons absorbed by the crystal per

second, which was just the number per second incident on the crystal minus the small (measured) fraction reflected. The carrier lifetime was determined as a function of laser power, and was defined to be the number of excess carriers excited at steady state (after a few msec) divided by the generation rate, $\tau = \Delta N / G$. Typical photoconductivity measurements are shown in Fig. 5 for an InP(100) sample. The steady-state differences in conductance are easily extracted from these results. Figure 6 shows the lifetime data for the same InP(100) crystal under two different surface conditions. The data shown in Fig. 5 provided the lettered points as indicated. The fit to the data is that suggested by Landsberg:¹³

$$1/\tau = 1/\tau_{\text{SRH}} + a_1 n + a_2 n^2, \quad (2)$$

where τ is the measured lifetime, n is the bulk-averaged excess carrier density, and a_1 , a_2 , and τ_{SRH} are constants fit to the data. The solid points of Fig. 6 show results from a Xe-cleaned annealed (but still somewhat contaminated, see Ref. 4) InP(100) crystal. The open points show the same crystal after cleaning with a dose of 10^{16} Xe at 14 eV and 70° incidence without a subsequent anneal. The solid and dashed curves show the fits of Eq. (2) to the solid and open points, respectively. This Xe processing is expected to create defects at the surface³ which function as traps and thus increase the surface recombination velocity and decrease the measured carrier lifetime. This effect is seen in Fig. 6 in which the measured lifetime dropped orders of magnitude after this low-energy sputter.

The Shockley-Read-Hall (SRH) lifetime, τ_{SRH} , corresponds to the lifetime at low excess carrier density, in the pseudo-first-order regime (where the lifetime remains nearly constant with increasing carrier density). Since the collisional excitation of e^-h^+ pairs produces relatively low excess carrier densities, only the SRH lifetimes will be considered here.

The SRH lifetime can be used to determine the surface recombination velocity (S):¹⁴

$$\tau_{\text{SRH}} = \frac{L_p \{ (D_p/L_p) \sinh(z/L_p) + S [\cosh(z/L_p) - 1] \}}{[S^2 + (D_p/L_p)^2] \sinh(z/L_p) + (2SD_p/L_p) \cosh(z/L_p)}, \quad (3)$$

where z is the crystal thickness (in cm), D_p is the diffusion constant for holes (in cm^2), and L_p is the hole diffusion length (in cm). Since the minority carrier lifetimes are measured and Fe-compensated InP is n type, we only consider hole diffusion. The diffusion constant can be determined from the hole mobility (μ_p) by the Einstein relation $D_p = \mu_p kT/e$, which for room temperature and the hole mobility of InP, $\mu_p = 150 \text{ cm}^2/\text{V sec}$,¹⁵ gives $D_p = 3.9 \text{ cm}^2/\text{sec}$. The diffusion length is then $L_p = (D_p \tau_B)^{1/2}$ where τ_B is the bulk lifetime of holes. The longest bulk-averaged SRH lifetime we observed on InP(100) was $3 \mu\text{sec}$. If we take this to be the bulk lifetime of holes (it is within the range of values found in the literature), then the hole diffusion length is $L_p = 0.0034$

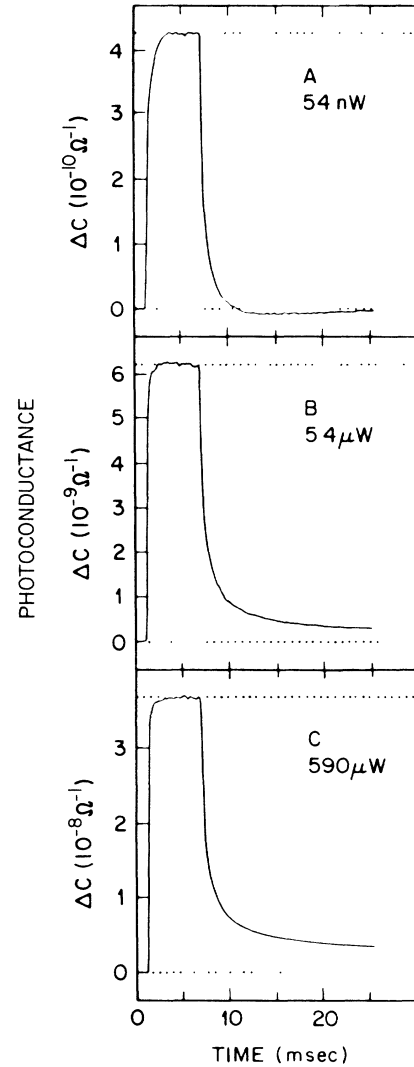


FIG. 5. Photoconductance of an InP(100) crystal as a function of time for a few-msec pulse of 442-nm light from a He-Cd laser for the incident laser powers indicated.

cm. This is much larger than the $\sim 0.05\text{-}\mu\text{m}$ penetration depth of the light from the He-Cd laser.¹⁶ Thus the steady state carrier distributions resulting from collisional and optical excitations were similar.

For an ordered InP(110) surface both collision-induced e^-h^+ excitation and optically excited carrier lifetime were measured. The bulk-averaged minority-carrier (hole) lifetime at low laser power was 50 nsec . Solving (3) iteratively gives a surface recombination velocity of $S = 67000 \text{ cm/sec}$. In this case, surface recombination dominates the sample-recombination rate as the bulk lifetime is $\tau_B \geq 3 \mu\text{sec}$ from above.

The surface-recombination velocity can be used to estimate the surface trap density (N_t) by¹⁷

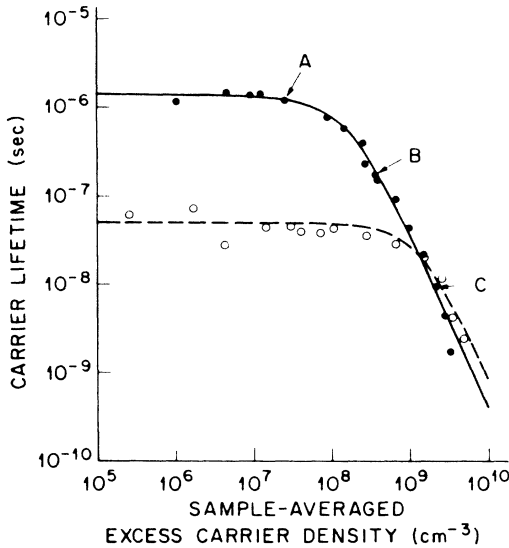


FIG. 6. Effective minority-carrier lifetime as a function of sample-averaged excess carrier density measured for InP(100) with two different surface preparations as described in the text. The lettered data points correspond to the photoconductance measurements shown in Fig. 5. The solid and dashed lines show the fits of Eq. (2) to the solid and open points, respectively.

$$S = \frac{(K_n K_p)^{1/2} (n_b + p_b) N_t}{2n_i \{ \cosh[(E_t^f - E_i)/kT - u_0] + \cosh(u_s - u_0) \}} \quad (4)$$

where K_n and K_p are the probabilities per unit time that an electron and a hole, respectively, will be captured by a vacant surface trap, n_b and p_b are the electron and hole bulk densities, respectively, n_i is the intrinsic carrier density, E_t^f is the effective trap energy level, E_i is the intrinsic Fermi energy, u_s is the difference of the surface Fermi energy and E_i divided by kT , and $u_0 = \ln[(K_p/K_n)^{1/2}]$. If it is assumed that electron and hole trapping probabilities are equal ($K_p = K_n$), then $u_0 = 0$, and the recombination can be described by the product of a cross section (σ_t in cm^2) and a thermal carrier velocity (v_t in cm/sec), $(K_n K_p)^{1/2} = \sigma_t v_t$. A lower limit can be derived for the surface trap density by zeroing both the arguments of the cosh terms in the denominator of (4). Rearranging we get

$$N_t \geq \frac{4n_i S}{(n_b + p_b) \sigma_t v_t} \quad (5)$$

Using the values of n_b and p_b derived from the conductivity of the sample, n_i for InP, typical values for $\sigma_t \approx 10^{-15} \text{ cm}^2$ and $v_t \approx 10^7 \text{ cm}/\text{sec}$, and the value derived for $S = 67\,000 \text{ cm}/\text{sec}$ gives a lower limit of the trap density $N_t \geq 7 \times 10^{10} \text{ cm}^{-2}$. An estimate can be made for the trap density by assuming that the effective trap energy lies at the measured surface Fermi-level position,⁹ so that $(E_t^f - E_i)/kT = u_s = 6$. If it is still assumed that $u_0 = 0$, then from (4) the derived surface trap density is $N_t \approx 1.4 \times 10^{13} \text{ cm}^{-2}$. The density of the InP(110) surface

is $4.1 \times 10^{14} \text{ atoms}/\text{cm}^2$, suggesting that on the order of $\frac{1}{30}$ of the surface sites are functioning as traps. These defect densities are not inconsistent with the sharp LEED patterns we observed.

2. Calibration of collisional e^-h^+ excitation

In both the collisional and optical carrier excitations, it is the bulk-averaged change in conductance that is measured. We assume that the only difference in the measured yield between the two types of excitation is due to the carriers collisionally excited and immediately trapped at the surface.¹⁸ Because of this, the measured yield provides a lower limit on the excitation probability.

The yield of the carrier excitation per incident Xe atom is defined to be

$$Y = G / F_{\text{Xe}} \quad (6)$$

where G is the e^-h^+ generation rate, and F_{Xe} is the Xe atom flux. At steady state, the generation rate and recombination rate are equal, so that the excess carrier density (ΔN) is determined by the generation rate and the carrier lifetime (τ):

$$\Delta N = G \tau \quad (7)$$

We use the lifetime as derived from the optical-excitation experiment at low excess carrier density and the known generation rate. We assume this lifetime can be used to derive the collision-induced generation rate. What is actually measured is a change in conductance, which is related by a geometrical factor to the change in conductivity ($\Delta\sigma$). The change in conductivity is

$$\Delta\sigma = q\mu\Delta N \quad (8)$$

where q is the charge of a carrier, and μ is the mobility of a carrier. For μ , the sum of the electron and hole mobilities for InP, $5000 \text{ cm}^2/\text{V sec}$, will be taken. Combining Eqs. (6)–(8), the yield so defined is

$$Y = \frac{\Delta\sigma}{q\mu\tau F_{\text{Xe}}} \quad (9)$$

For an ordered InP(110) surface the collisional e^-h^+ yield was measured and concurrently a minority carrier lifetime of 50 nsec at low excess carrier density was determined by optical excitation. Using these measured values, the experimentally derived collisional excitation yield for Xe at 9.8 eV is $Y = 0.002$. This value is smaller than the order-of-magnitude estimate of Ref. 2 for InP(100), despite the comparable flux-normalized e^-h^+ yields, because a fast value for the carrier lifetime was assumed in the previous work.

If it is assumed that carriers are equilibrated to the local lattice energy, it is possible to use the measured yield to determine the effective number of degrees of freedom over which the deposited energy is dissipated in order to achieve the carrier excitation probability observed.² Referring to Fig. 4, the experimental dependence of the e^-h^+ signal on ΔE^{-1} , the Boltzmann fraction of carriers that will be excited above the band gap, is assumed to be described by

$$Y = A \exp(-3nE_{BG}/\Delta E_{Xe}), \quad (10)$$

where E_{BG} is the band gap of InP, 1.35 eV, and n is the effective number of atoms participating in the equilibration. The high-temperature heat capacity $C_v = 3nk$ has been used. From the slope of the solid line in Fig. 4 for InP(100), 31.6 eV, the value of n can be determined: $n = 31.6 \text{ eV}/(3E_{BG}) = 8$ atoms.¹⁹ Note that this small number is consistent with the idea of a *local* containment of the energy transfer for carrier excitation yield. The temperature change from which the electronic equilibration was established is determined by simply dividing the energy deposited by the heat capacity $\Delta T = \Delta E_{Xe}/3nk$, which for an incident energy of 9.8 eV, and an assumed energy transfer $\Delta E = 8 \text{ eV}$, gives a temperature rise of 3900 K. From the effective number of lattice atoms derived from the energy dependence of the InP(100) data, and the calibrated yield at 9.8 eV for InP(110), the value of the preexponential is $A = 0.002 \exp(3nE_{BG}/8) = 0.11$. That is, we have used the optically derived lifetime for the InP(110) crystal and the slope of the Boltzmann plot for the InP(100) crystal to derive this value for the preexponential. As the measured excitation yields were approximately the same for both the InP(100) and InP(110) crystal surfaces this should be a valid estimate of the value of the preexponential.

The preexponential, A of Eq. (10), can be approximated by the intrinsic carrier concentration at the effective temperature for this volume of eight atoms:

$$A = 2 \left[\frac{2\pi(m_e^* m_h^*)^{1/2} kT}{h^2} \right]^{3/2} V_n, \quad (11)$$

where m_e^* and m_h^* are the effective masses of the electron and hole, respectively, T is the (effective) temperature, and V_n is the volume taken up by the n atoms involved. Taking $m_e^* = 0.077m_e$ and $m_h^* = 0.8m_e$,^{15]} $T = 4200 \text{ K}$ from above, and the volume of $n = 8$ atoms for InP [$\rho = 4.787 \text{ g/cm}^3$ (Ref. 15)] to be $V_8 = 4.635 \times 10^{-12} \text{ cm}^3$ gives $A = 0.66$.

Nearly the same, the preexponential A applies by analogy to the thermodynamic equilibrium responsible for the ionization of atoms, for which the preexponential that would be expected is^{20,21}

$$A = 2 \frac{g_1^+}{g_k} \left[\frac{2\pi m_e^* kT}{h^2} \right]^{3/2} V_n, \quad (12)$$

where g_k and g_1^+ are the degeneracies of the ground and ionized states, respectively, and the other terms are defined above.²² The formulas are the same except for the mass dependence which differs by a factor of 5.8. Taking the same values used above, and assuming 1 for the ratio of the degeneracies, gives $A = 0.11$.

Either of these estimates ($A = 0.66, 0.11$) agrees well within the uncertainties of the arguments with the value derived from the experiments ($A = 0.11$) and serves to show the consistency of a local thermal hot-spot description with the experimental results.

3. Further study of carrier recombination kinetics

It is possible to extract some qualitative features of the carrier recombination kinetics from the conductivity waveforms of the optically excited carriers by transforming into the frequency domain. The result of the transform is called the transfer function and is the imaginary part of the Fourier transform as a function of the real part. This method of analysis of reaction rates in the frequency domain is well established in the field of surface chemical reaction kinetics,^{23–25} as well as in other fields of physical sciences.^{26,27} In particular, the shape of the transfer function is characteristic of the operative kinetics of a rate process. Examples of transfer functions for a variety of kinetics are given in Ref. 25.²⁸ A comparison is usually made with a semicircle with its center on the real axis going through the first Fourier component in a plot of the Argand (complex) plane. This semicircle, also called a Cole-Cole plot, represents the transfer function obtained for a single first-order rate process.²⁷ More complicated kinetics lead to characteristic deviation from this semicircle as discussed in Ref. 25.

Typical examples of transfer functions obtained are shown in Fig. 7 which are those associated with the waveforms in Fig. 5. Note that the kinetics of the rise and fall in photoconductance are different in each case. Also, the shape of these plots indicate that there are mul-

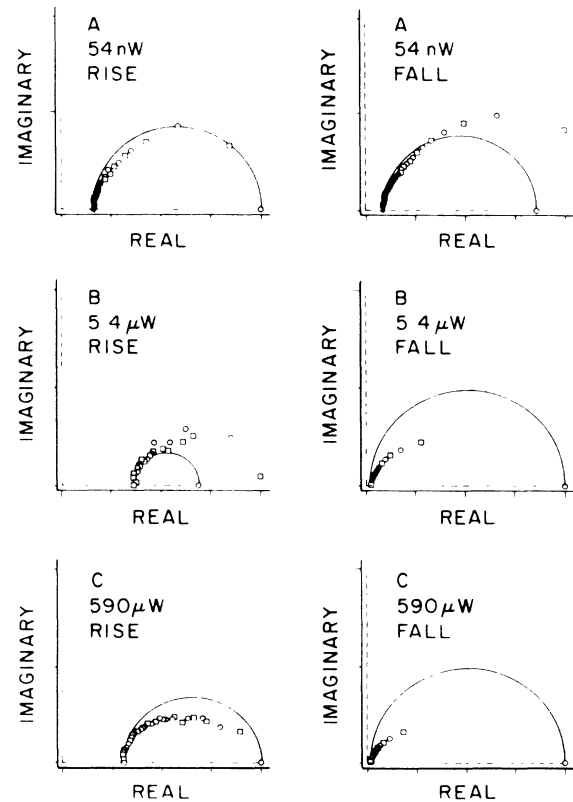


FIG. 7. Argand plane plots of the transfer functions for the rise and fall of the photoconductance in the data of Fig. 5 as indicated. The semicircles in each plot are what would be expected if the rise or fall were determined by a single first-order process.

multiple competing rates in both the rises and falls in conductivity. This is seen as the flattening of the transfer functions to values lower than the indicated semicircles, and also by the dips evident in the plots, which can be ascribed to competing (parallel) rate processes.²⁵

As an example of the complexities associated with carrier recombination rates we discuss one of several interesting features observed in the photoconductance traces—the dip below the equilibrium (dark) conductance after the laser is turned off in Fig. 5(a) which was often seen at low laser power. This overshoot leads to the lobe protruding out of the side of the semicircle in the transfer function plot in the “FALL” section of Fig 7(a). We hypothesize the following explanation. The Fe-compensated semi-insulating InP samples used were *n*-type. From studies of the effects of adsorption on the samples with our surface-preparation procedure, we observe an accumulation layer, that is the bands were bent down leading to excess surface conductivity.⁹ If the excess population in surface states with a net negative charge (acceptor states) decays more slowly than the excess population in surface states with a net positive charge (donor states), and if the optically excited carriers have decayed sufficiently, then the band-bending changes can reduce the conductivity to below its equilibrium value.

One conclusion from the observation of this feature is that the decay of the photoconductivity generated by a brief pulse of light may give misleading results in the case where surface trapping and band bending are important processes. It should also be pointed out that the lifetimes derived from the steady-state measurements are certainly affected by band bending. Some estimate of the magnitude of this effect can be made by looking at the various overshoots and peaks observed in the photoconductance traces. All of these are under 10% of the steady-state photoconductance, which is smaller than the probable (systematic) error in the derived lifetimes. In the case of the data used for the calibration of the collisional excitation of carriers, however, it was determined that the band bending was reduced to relatively low values.⁹

C. Other experiments

Although in Ref. 2 a sensitive apparatus for detecting collision-induced luminescence was put in place, none was observed. From the carrier recombination lifetimes determined above, one can make an estimate of how many photons would be expected from these collisions. The excess carrier density is known from the transient conductivity. An upper limit for the radiative recombination rate is if all carriers had decayed radiatively in the photoconductivity or recombination studies. The

lower limit of the bulk lifetime was measured to be 3 μ sec, giving an upper limit of the radiative recombination rate of $3 \times 10^5 \text{ sec}^{-1}$. The actual radiative recombination rate would be expected to be far lower than this. At the band gap, the absorption coefficient of InP is $\sim 1 \times 10^4 \text{ cm}^{-1}$,¹⁶ so only photons emitted in the top $\sim 1 \mu\text{m}$ are detectable. The area illuminated by the Xe beam was 0.02 cm^2 . This implies that for the largest transient current signals, where there were $1.6 \times 10^6 \text{ cm}^{-3}$ excess carriers near the surface (using the hole diffusion length of 0.0034 cm calculated above), one would expect fewer than $10^6 \text{ photons sec}^{-1}$, which is below the limit of the sensitivity of the experiment conducted.

We were unable to observe any collisionally excited e^-h^+ on either the Si(100) or the Si(111) surface. The sensitivity was low in these experiments due to the relatively low resistivity ($1500\text{--}3000 \Omega \text{ cm}$) of the Si samples. We suggest the combination of this low sensitivity and the likelihood of high surface-recombination velocities account for the lack of any observable effect. Comparable collision-induced e^-h^+ yields were obtained on the ordered InP(110) and the somewhat disordered InP(100) surfaces. In addition, using an ultrapure rectified *p-i-n* Ge(100) diode, collision-induced e^-h^+ generation was observed of comparable magnitude.¹ The generic description of the excitation process and comparable results for these surfaces imply that electronic excitations occur similarly on the elemental semiconductor surfaces, but their measurement as carriers by conductivity change may be more difficult.

IV. SUMMARY

We have extended our experiments and description of the excitation of carriers at semiconductor single-crystal surfaces. The excitation of carriers at the surface of InP(110) was measured to be comparable to that of InP(100). Using an optical technique to determine effective carrier lifetimes, the yield was found to be $0.002 e^-h^+$ per incident Xe atom at Xe energies of 9.8 eV at normal incidence on InP(110). The excitation occurred in a manner consistent with electronic equilibration with the initial local lattice energy in the immediate vicinity of the impact.

ACKNOWLEDGMENTS

The authors would like to thank Ami Applebaum, Vince Lambrecht, Murray Robbins, and Peter Thomas for evaporating contacts on the InP crystals, Ed Chaban for assistance in setting up the experiments, Dave Allara for the loan of a He-Cd laser, and Greg Blonder, Si Glarum, Michel Lannoo, Mark Stiles, and John Tully for helpful discussions.

*Present address: IBM Research, Almaden Research Center, San Jose, CA 95120.

¹A. Amirav, W. R. Lambert, M. J. Cardillo, P. L. Trevor, P. N. Luke, and E. E. Haller, *J. Appl. Phys.* **59**, 2213 (1986).

²A. Amirav and M. J. Cardillo, *Phys. Rev. Lett.* **57**, 2299 (1986).

³A. Amirav and M. J. Cardillo, *Surf. Sci.* **198**, 192 (1988).

⁴P. S. Weiss, A. Amirav, P. L. Trevor, and M. J. Cardillo, *J. Vac. Sci. Technol. A* **6**, 889 (1988).

⁵A. Amirav, M. J. Cardillo, P. L. Trevor, C. Lim, and J. C. Tully, *J. Chem. Phys.* **87**, 1796 (1987).

- ⁶C. Lim, J. C. Tully, A. Amirav, P. Trevor, and M. J. Cardillo, *J. Chem. Phys.* **87**, 1808 (1987).
- ⁷M. J. Cardillo, C. C. Ching, E. F. Greene, and G. E. Becker, *J. Vac. Sci. Technol.* **15**, 423 (1978).
- ⁸J. C. Tsang, A. Kahn, and P. Mark, *Surf. Sci.* **97**, 119 (1980).
- ⁹P. S. Weiss, P. L. Trevor, and M. J. Cardillo (unpublished).
- ¹⁰S. M. Sze, *Semiconductor Devices, Physics and Technology* (Wiley, New York, 1985), p. 47.
- ¹¹The value of the energy transfer for each set of data was taken as the difference of the incident energy and the energy corresponding to the peak of the time of flight of the scattered atom, which was in all cases close to the mean energy transfer.
- ¹²Caution should be exercised in the relation of mean incident energy and mean energy transfer to the efficiencies of relatively improbable events, because these events may be due only to certain unrepresentative collisions or to conditions far out in the wings of the incident distributions. In the cases here, however, the systematics indicate that this is not a problem.
- ¹³P. T. Landsberg, *Appl. Phys. Lett.* **50**, 745 (1987). This functional form is used for convenience, and its use is not meant to imply that the underlying physics are the same here.
- ¹⁴A. Many, Y. Goldstein, and N. B. Grover, *Semiconductor Surfaces* (North-Holland Amsterdam, 1965), p. 260.
- ¹⁵M. Neuberger, *Handbook of Electronic Materials*, Vol. 2 of *III-V Semiconducting Compounds* (IFI/Plenum, New York, 1971).
- ¹⁶H. Burkhard, H. W. Dinges, and E. Kuphal, *J. Appl. Phys.* **53**, 655 (1982).
- ¹⁷A. Many, Y. Goldstein, and N. B. Grover, *Semiconductor Surfaces*, Ref. 14, p. 197.
- ¹⁸It should be noted that it has not previously been necessary to distinguish between the outermost atomic layer and the first few underlying layers in terms of their contribution to the surface-recombination velocity. Although the unsatisfied bonds due to termination of the bulk are at the outermost layer, the contribution of the next few layers is not well separated. The trap density estimated above is thus a projection onto the surface of the trap density on and near the surface. If it is necessary to separate out those carriers that initially escape the surface in order to be detected, this is important. The effects of immediate trapping upon excitation have been neglected here.
- ¹⁹This slope is the same whether or not the measured widths of the incident-energy distributions are taken into account. The effect of the deconvolution of the incident-energy distribution is to shift the least-squares line fit to the data down by 0.15 units on the logarithmic scale of Fig. 4. The Xe and Kr atoms are thus 15% less effective at each energy at exciting $e^{-}h^{+}$ pairs than the fit would indicate.
- ²⁰M. Mitchner and C. H. Kruger, Jr., *Partially Ionized Gases* (Wiley, New York, 1973).
- ²¹D. H. Menzel, *Proc. Natl. Acad. Sci. U.S.A.* **19**, 40 (1933).
- ²²The reduced mass of the electron-hole pair would be most correct, but since the effective hole mass in InP (0.8) is an order of magnitude larger than the effective electron mass (0.077) (Ref. 15), the reduced mass is essentially the same as the effective electron mass.
- ²³R. H. Jones, D. R. Olander, W. J. Siekhaus, and J. A. Schwarz, *J. Vac. Sci. Technol.* **9**, 1429 (1972).
- ²⁴C. T. Foxon, M. R. Boudry, and B. A. Joyce, *Surf. Sci.* **44**, 69 (1974).
- ²⁵H. Sawin and R. P. Merrill, *J. Vac. Sci. Technol.* **19**, 40 (1981).
- ²⁶G. L. Miller, D. V. Lang, and L. C. Kimerling, *Annu. Rev. Mater. Sci.* **7**, 377 (1977).
- ²⁷K. S. Cole and R. H. Cole, *J. Chem. Phys.* **9**, 341 (1941).
- ²⁸The examples of Ref. 25 are instructive, but one correction should be noted: for parallel branched first-order kinetics, the symmetric transfer function plots shown are obtained only for branching ratios of $p = k_1/k_2$ where $k_2 > k_1$ (not $p = 0.5$ in general).